Degassing dynamics of basaltic lava lake at a top-ranking volatile emitter: Ambrym volcano, Vanuatu arc

Patrick Allard, Mike Burton, Georgina Sawyer, Philipson Bani

Earth and Planetary Science Letters 448 (2016) 69–80

Contents lists available at ScienceDirect

Earth and Planetary Science Letters

www.elsevier.com/locate/epsl

Degassing dynamics of basaltic lava lake at a top-ranking volatile emitter: Ambrym volcano, Vanuatu arc

Patrick Allard [a,b,*], Mike Burton [c], Georgina Sawyer [d], Philipson Bani [e]

[a] Institut de Physique du Globe de Paris, UMR7154 CNRS, Paris, France
[b] Istituto Nazionale di Geofisica e Vulcanologia, Catania, Italy
[c] SEAES, University of Manchester, United Kingdom
[d] Department of Geography, University of Cambridge, United Kingdom
[e] IRD, Laboratoire Magmas & Volcans, Clermont-Ferrand, France

ARTICLE INFO

Article history:
Received 10 September 2015
Received in revised form 7 May 2016
Accepted 9 May 2016
Available online xxxx
Editor: T.A. Mather

Keywords:
Ambrym
lava lake
infrared spectroscopy
volcanic gases
magma degassing dynamics
volatile fluxes

ABSTRACT

Persistent lava lakes are rare on Earth and provide volcanologists with a remarkable opportunity to directly investigate magma dynamics and degassing at the open air. Ambrym volcano, in Vanuatu, is one of the very few basaltic arc volcanoes displaying such an activity and voluminous gas emission, but whose study has long remained hampered by challenging accessibility. Here we report the first high temporal resolution (every 5 s) measurements of vigorous lava lake degassing inside its 300 m deep Benbow crater using OP-FTIR spectroscopy. Our results reveal a highly dynamic degassing pattern involving (i) recurrent (100–200 s) short-period oscillations of the volcanic gas composition and temperature, correlating with pulsated gas emission and sourced in the upper part of the lava lake, (ii) a continuous long period (~8 min) modulation probably due to the influx of fresh magma at the bottom of the lake, and (iii) discrete CO_2 spike events occurring in coincidence with the sequential bursting of meter-sized bubbles, which indicates the separate ascent of large gas bubbles or slugs in a feeder conduit with estimated diameter of 6 ± 1 m. This complex degassing pattern, measured with unprecedented detail and involving both coupled and decoupled magma-gas ascent over short time scales, markedly differs from that of quieter lava lakes at Erebus and Kilauea. It can be accounted for by a modest size of Benbow lava lake and its very high basalt supply rate (~20 $m^3 s^{-1}$), favouring its rapid overturn and renewal. We verify a typical basaltic arc signature for Ambrym volcanic gas and, based on contemporaneous SO_2 flux measurements, we evaluate huge emission rates of 160 Gg d^{-1} of H_2O, ~10 Gg d^{-1} of CO_2 and ~8 Gg d^{-1} of total acid gas (SO_2, HCl and HF) during medium activity of the volcano in 2008. Such rates make Ambrym one of the three most powerful volcanic gas emitters at global scale, whose atmospheric impact at local and regional scale may be considerable.

1. Introduction

Persistent lava lake activity, occurring at rare volcanoes worldwide, is a remarkable phenomenon where molten magma steadily supplied to an open reservoir degases directly into the atmosphere from across its surface, while loosing little to no solid mass (e.g. Le Guern et al., 1979; Tazieff, 1994; Oppenheimer et al., 2004, 2009). Such an activity, which can persist for decades (e.g. at Kilauea and Erebus volcanoes) to more than a century (Nyiragongo and Erta'Ale volcanoes), is of great value in volcanological research as it exposes what is normally hidden within persistently active volcanoes: the innermost magma dynamics capable to sustain continuous gas and heat flow. Its study therefore permits direct comparison between measured geophysical and geochemical parameters and volcanic activity, allowing features such as magma convection, passive degassing, lava fountains or explosive gas bubbling to be understood in a quantitative framework.

Because degassing contributes most of the total mass output from a lava lake, key insights into the processes controlling this rare volcanic activity can be obtained by measuring the chemistry and flux of magmatic gas emissions. Gas fluxes provide quantitative constraints on the rates of magma supply and convection, while gas compositions provide constraints upon the degassing mechanisms and their source depth if the abundance and behaviour of volatiles in the magma are known (e.g. Allard et al., 2005; Oppenheimer et al., 2009; Beckett et al., 2014). Efficient con-

* Corresponding author at: Institut de Physique du Globe de Paris, UMR7154 CNRS, Paris Sorbonne Cité, France.
E-mail address: pallard@ipgp.fr (P. Allard).

http://dx.doi.org/10.1016/j.epsl.2016.05.014
0012-821X/

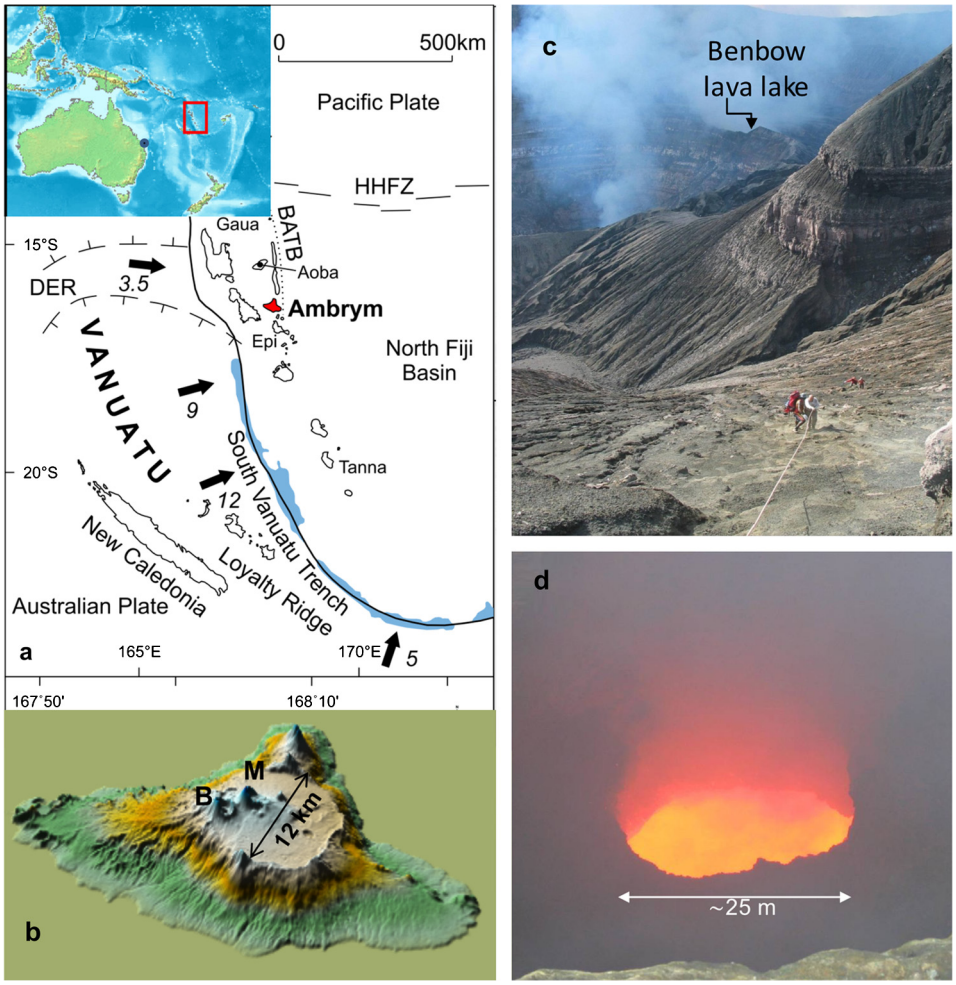

Fig. 1. Ambrym volcano and its degassing lava lake in Benbow crater. (a) Location of Ambrym volcano in the central part of Vanuatu island arc, affected by collision with the D'Entrecasteaux Ridge (DER) (modified from Allard et al., 2015). The insert shows the location of Vanuatu arc with respect to Australia and to the Cap Ferguson CSIRO air monitoring station (19.28°S, 147.05°E; see section 3); (b) Digital elevation model of Ambrym island showing the summit caldera and the two main active cones, Benbow (B) and Marum (M); (c) Inner structure of Benbow cone viewed from its southeast rim and location of its active lava lake in 2007–2008; (d) Degassing Benbow lava lake (~25 m wide). Photo credit: P. Allard.

vective magma overturn in lava lake-conduit systems, with gravitational sinking of the unerupted degassed magma, is strongly required from heat and mass balances (e.g. Tazieff, 1994; Kazahaya et al., 1994; Stevenson and Blake, 1998; Harris et al., 1999; Oppenheimer et al., 2004, 2009; Beckett et al., 2014). It is also supported by theoretical modelling (Witham and Llewellin, 2006) and cyclic crystal zonation in erupted solid products (Moussallam et al., 2015). However, separate bubble flow is another mechanism able to carry heat and gas to a lava lake (Bouche et al., 2010) and to control its level oscillations through bubble accumulation at its top (Patrick et al., 2016). Variations in magma-gas supply rates, degassing modes and the style of convection actually determine a wide range in lava lake behaviour, from vigorous bubbling and overturn to quieter degassing and resurfacing, interrupted or not by recurrent gas outbursts (e.g. Le Guern et al., 1979; Tazieff, 1994; Oppenheimer et al., 2004, 2009), and to cyclic upheaval and drain back due to gas-piston effects (Edmonds and Gerlach, 2007; Patrick et al., 2016).

The composition and mass output of magmatic gases from a lava lake can be measured using up-to-date spectroscopic methods. In the past fifteen years, open-path Fourier transform infrared (OP-FTIR) spectroscopy has been demonstrated to be a remarkable tool for remotely quantifying magmatic gas compositions during effusive and explosive eruptions at high frequency and from a safe position (e.g. Allard et al., 2005; Burton et al., 2007a; La Spina et al., 2015). Using infrared radiation emitted by molten lava, OP-FTIR absorption spectroscopy allows simultaneous determination of the principal components of hot volcanic gases: H_2O, CO_2, SO_2, HCl, HF, CO, apart from H_2 and H_2S. Therefore, this tool is particularly well-suited to study the degassing of lava lakes. It has already been applied to study gas emissions from the exceptional long-lived lava lakes hosted by Nyiragongo on the East-African Rift (Sawyer et al., 2008a), Erta'Ale in Ethiopia (Sawyer et al., 2008b), Erebus in Antarctica (Oppenheimer and Kyle, 2008; Oppenheimer et al., 2009; Ilanko et al., 2015) and Kilauea in Hawaii (Edmonds and Gerlach, 2007; Edmonds et al., 2013; Patrick et al., 2016). These four volcanoes, located on either hot spots or rift zones, are fuelled by magmas ranging in composition from basalt (Kilauea, Erta'Ale) to nephelinite (Nyiragongo) and phonolite (Erebus), which is reflected in widely differing gas compositions. OP-FTIR spectroscopy has also been applied on two of the rare basaltic to andesitic volcanoes in subduction zones where lava lakes have been observed to recurrently form and persist: Masaya in Nicaragua (Burton et al., 2000) and Villarrica in Chile (Sawyer et al., 2011). However, until now comprehensive OP-FTIR investigation of the degassing dynamics of a lava lake has been achieved only on Erebus (Oppenheimer et al., 2009; Ilanko et al., 2015) and Kilauea (Edmonds and Gerlach, 2007; Edmonds et al., 2013; Patrick et al., 2016), where long or detailed enough series of measurements could be realized.

Here we report on the first OP-FTIR study of the dynamics of lava lake degassing at Ambrym, in Vanuatu, a remarkable basaltic arc volcano displaying such an activity and intense gas emissions in the southwest Pacific region. Ambrym island, located in the central part of Vanuatu arc (Fig. 1a), is the subaerial exposure of a massive (~500 km^3) basaltic shield volcano rising 1800 m above the sea floor. At its summit, a 12-km wide caldera which formed about 2 ka ago (MacCall et al., 1970) hosts two large active cones, Benbow and Marum (Fig. 1b), where the degassing of recurrent lava lakes sustains voluminous gas release. Because of the remote location of the volcano, challenging access to its vents and adverse tropical weather conditions, this activity has long remained unstudied. The very first airborne and ground-based measurements, performed in 2005–2007, revealed prodigious gas emission rates from Ambrym (Bani et al., 2009, 2012; Allard et al., 2015), ranking it amongst the strongest persistent emitters of volcanic volatiles on Earth (Allard et al., 2015). However, no high temporal resolution data were collected in these studies.

In October 2008 we therefore conducted OP-FTIR spectroscopic measurements on Ambrym in order to measure the dynamics of its lava lake activity at high temporal resolution. Our measurements were made from the shortest possible distance to the lava lake that was actively degassing for ~1.5 yr at the bottom of its ~300 m deep Benbow vent, and volcanic gas composition was retrieved every 5 s. While providing new constraints on Ambrym gas chemistry, our results reveal short-term oscillations in volcanic gas composition, with different periodicities, that track a highly dynamic degassing pattern of the lava lake. Morlet wavelet analysis of these compositional variations is combined with our field observations and melt inclusion data for dissolved volatiles (Allard et al., 2015) to infer the magmatic processes controlling this degassing pattern. Moreover, by combining our OP-FTIR data set with the SO_2 plume flux determined from contemporaneous airborne UV sensing we quantify the gas emission rates. The results, discussed in comparison with data for other lava lakes in different geodynamic contexts, confirm Ambrym volcano's status as one of the three most powerful persistent emitters of magmatic volatiles on Earth. Hence, our study provides new information on the high frequency dynamics of lava lake degassing at a top-ranking arc emitter of basaltic gases, and further insights into magma dynamics at basaltic volcanoes in general.

2. Volcanic activity and methodology

Our measurements, on 5 October 2008, targeted the active lava lake that was vigorously degassing at the bottom of Ambrym's Benbow cone (1160 m elevation a.s.l. and ~300 m deep). In order to determine magmatic gas compositions with OP-FTIR spectroscopy, we climbed down the eastern inner wall of the cone with our equipment (Fig. 1c) then climbed across the eastern edge of the crater terrace before reaching the northern pit crater (815 m a.s.l.) hosting the lake. It is the first time OP-FTIR spectroscopy was operated so deeply inside a volcanic vent. The lava lake was ponding at ~110 m depth in the southern part of the pit, a few meters lower than the crater floor (Figs. 1d), as measured with laser range-finding binoculars. It was approximately circular, with a diameter of ~25 m, but possibly extended more widely under the crater floor (Fig. 2). Even though concentrated gas fumes sometimes obscured its viewing, we could observe that the overall lava lake surface was repeatedly turned over by vigorous spattering, associated with a pulsated degassing (puffs), and, intermittently, by the sequential bursting of very large (meter-sized) gas bubbles. Otherwise, its level remained broadly stable during our measurements.

We positioned our spectrometer, its controlling laptop and a 12 V DC powering battery on the northern rim of the pit

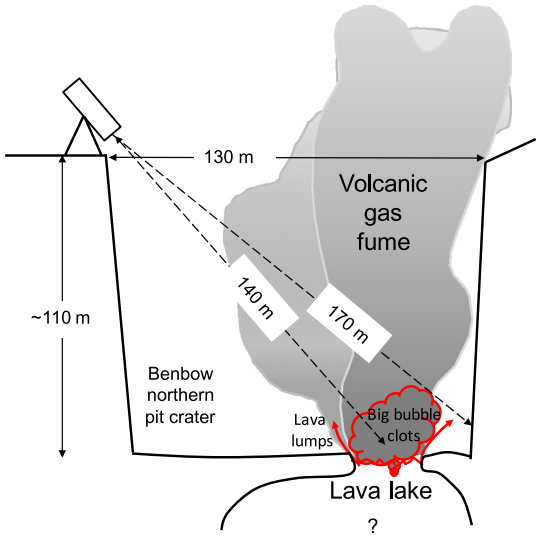

Fig. 2. Schematic drawing of OP-FTIR spectroscopic measuring conditions at the bottom of Benbow crater in October 2008. Distances were measured with laser range-finding binoculars (Wilco LRB 4000-VCE). Slanting distance from our spectrometer to the centre of lava lake averaged 140 ± 10 m. The spectrometer was inclined on its tripod at an angle of 58° below horizontal and, given its 20 mrad field of view, measured IR radiation emitted by a ~7 m^2 area of the degassing lake. The southern crater wall behind the lava lake was distant by 170 m. The drawing illustrates the ejection of lava lumps, sometimes reaching the crater floor, and the intermittent sequential bursting of very large (meter-sized) gas bubbles.

(16°15.312S and 168°06.240E), outside the volcanic gas plume. The spectrometer, occasionally realigned to optimize viewing around a mobile dense gas plume, targeted the centre of the lava lake at an average slanting distance of 140 ± 10 m (Fig. 2). Its 20 mrad field of view allowed us to measure infrared radiation emitted by a ~7 ± 1 m^2 lake area. Our spectrometer was a MIDAC 4401-S equipped with a ZnSe beam splitter and a Stirling engine cooled MCT detector (avoiding the logistically challenging need of liquid nitrogen). The detector has a 600 to 5000 cm^{-1} sensitivity and 0.5 cm^{-1} resolution. Single-sided interferograms of the IR radiation emitted by molten lava and absorbed by atmospheric and volcanic gases were collected at a frequency of 1 Hz over a period of 1.6 h (except for a 20 min interruption due to rainfall). To improve the signal-to-noise ratio and hence the quality of recorded spectra, five consecutive interferograms were co-added and subsequently Fourier transformed by applying power spectrum phase correction and Norton–Beer medium apodization. We thus obtained 943 FTIR spectra of Benbow lava lake degassing at 5 s period.

Spectroscopic gas features were in absorption, indicating a lower temperature of the measured gas compared to the radiating source. They were analyzed following the retrieval procedures developed for OP-FTIR spectrum analysis (Burton et al., 2000), refined for higher temperature gases (Allard et al., 2005; La Spina et al., 2015). For each spectrum we retrieved the column amounts (expressed in units of molecules cm^{-2}) of eight IR-active gas species in the following wave bands: H_2O and CO_2 (2040–2165 cm^{-1}), SO_2 (2490–2550 cm^{-1}), HCl and CH_4 (2690–2810 cm^{-1}), HF (4035–4210 cm^{-1}), CO and N_2O (2145–2245 cm^{-1}). Gas column amounts were obtained from nonlinear least-squares best fitting (Rodgers, 1976's optimal estimation algorithm) between the measured spectra and simulated spectra based on the radiative transfer forward model of Edwards and Dudhia (1996) and infrared absorption line parameters from the HITRAN database (Rothman et al., 2005). The standard deviation of fitting residuals across the respective spectral windows yields an estimate of the error on the retrieved column amount of each gas, illustrated by error bars in the plots of Fig. 3. Radiative transfer in the two layers of hot

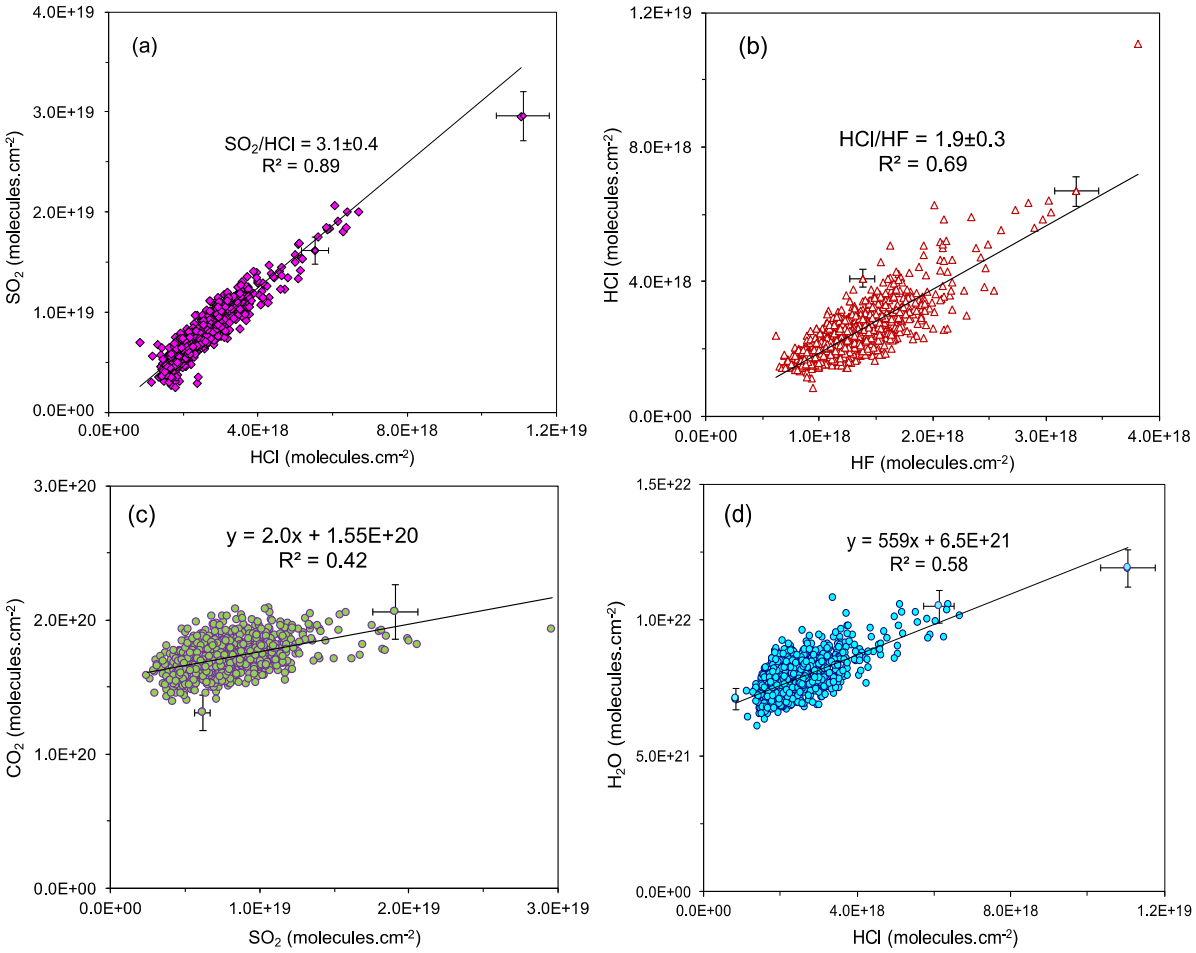

Fig. 3. a–d – Scatter plots of measured gas path amounts: (a) SO_2 versus HCl, (b) HCl versus HF, (c) CO_2 versus SO_2 and (d) H_2O versus HF. The gradient of linear regression in each plot defines the average molar ratio between the gas species in the pure volcanic gas. In Figs. 3c and 3d the y-intercept of regression line indicates the average background amount of CO_2 and H_2O in ambient air of the pit crater. Error bars indicates the overall uncertainty (1σ) for each species. See section 3.2.

volcanic gas and ambient atmospheric gases viewed by the spectrometer was calculated using the temperature of each layer. For the atmospheric layer we used the ambient temperature (292.6 K) and pressure (919 hPa) measured on site with a hand-held meteorological sensor. The temperature of the volcanic gas layer was determined for each spectrum from the highly T-dependent rotational band structure of SO_2 at 2500 cm^{-1} (Allard et al., 2005; Burton et al., 2007a). We also determined the temperature of the radiating source from the ratio of IR intensity recorded at 4400 and 4460 cm^{-1} and by fitting to a scaled Planck curve (Allard et al., 2005).

Our data time series for the volcanic gas amounts and gas ratios are depicted in Figs. 4 and 5. In order to identify and quantify possible degassing periodicities, we performed a continuous Morlet wavelet transform (CMWT) analysis of the gas ratios time series, using the code of Grinsted et al. (2004). CMWT analysis is particularly suitable for studying natural processes not stationary in time (Torrence and Combo, 1998), such as volcanic degassing (e.g. Tamburello et al., 2013; Ilanko et al., 2015); it permits to examine periodicities of a time series by moving and stretching a Morlet guide-wave and analyzing step-by-step its correlation with the signal. Wavelet power spectra reveal the strength of periodicities at different times and for different periods. Our data time series for Ambrym were close to normal distribution and thus did not require prior log-transformation. They were simply resampled at 1 Hz in order to get a time series with uniform step from 0 to 2885 s. The code of Grinsted et al. (2004) was used with the default parameters (e.g. automatic estimation of the background power spectrum, 1/12 octaves per scale) and result significance was assessed by assuming a red noise background, automatically modelled by a first order autoregressive (AR1) estimator. The code adds a cone of influence (COI) in which edge effects related to the length of the time series cannot be ignored. In our study this prevented from detecting periodicities lower than 6 s. We also checked the phase relationship between selected pairs of gas ratios by computing the coherence spectra between their wavelet transforms (Torrence and Compo, 1998). Results are displayed in Figs. 6 and 7 and discussed in section 4.2.

Finally, during our field campaign, on October 8, the bulk SO_2 plume flux from Ambrym and the respective flux contribution from Benbow and Marum craters were determined using airborne UV (DOAS) absorption spectroscopy. The results are reported in Allard et al. (2015). Combining these data with our OP-FTIR results therefore allows us to quantify both the single and total gas emission rates from Benbow crater and Ambrym in October 2008.

3. Results

3.1. Gas temperature and column amounts

The temperature of air-diluted Benbow volcanic gas was found to vary between 300 and 420 K, with a mean of 340 ± 20 K. Such low temperatures, compared to ~1400 K at emission from the molten basalt (section 4.2), demonstrate a rapid cooling of the magmatic gas upon emission and dilution by entrained ambient air. A higher mean temperature of 770 ± 120 K was determined for

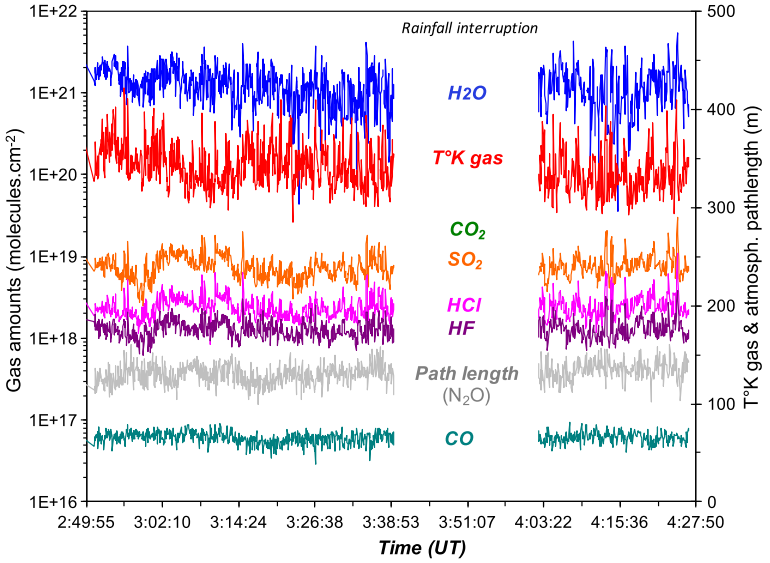

Fig. 4. Time series of the pure volcanic gas amounts, the gas temperature and the atmospheric optical path length for each spectrum during OP-FTIR measurement of Benbow lava lake degassing. H_2O, CO_2 and CO amounts are corrected for air dilution. Details on retrieval of the volcanic gas temperature and the atmospheric optical path length (deduced from the N_2O amount in each spectrum) are given in Sections 2 and 3. Note the co-variations of most gas species and temperature, anti-correlated with changes in the atmospheric optical path length, which track temporal variations in the thickness and density of the volcanic gas layer viewed by our spectrometer.

the radiating source, consistent with all spectra being in absorption. The mean thermal contrast of 330 K between the IR source and the volcanic gas warrants a negligible contribution of thermal emission from hot gases themselves in the spectral region of interest (>2000 cm^{-1}).

As previously mentioned, eight IR-active gas species (H_2O, CO_2, SO_2, HCl, HF, CO, CH_4 and N_2O) were retrieved in our spectra. The overall uncertainty on their amounts due to measurement and retrieval ranges between 4 and 7% for SO_2, HCl, and HF, 8–10% for H_2O, CO_2 and N_2O, and 10–12% for CO. CH_4, absent in hot basaltic gases and affected by a greater uncertainty, is left out in the following. Whilst SO_2, HCl and HF are purely volcanic in origin, H_2O, CO_2 and CO are both volcanic and atmospheric components, so their amounts must be corrected for air dilution. N_2O, which is purely atmospheric, is a reliable indicator for that correction. For the abundance of N_2O (0.32 ppmv) and other gases in Vanuatu's atmosphere in October 2008 we refer to the data recorded by the CSIRO air monitoring station of Cap Ferguson (http://www.csiro.au/greenhouse-gases/), eastern Australia, which is the closest station of the World Meteorological Organization (Fig. 1a).

Fig. 3 shows scatter plots of the bulk path amounts of (a) SO_2 versus HCl, (b) HCl versus HF, (c) CO_2 versus SO_2 and (d) H_2O versus HCl in our 943 spectra. In each plot the gradient of linear regression defines the average molar ratio of the species in the pure volcanic gas. The values are 3.1 ± 0.4 for SO_2/HCl, 1.9 ± 0.3 for HCl/HF, 2.0 ± 1.4 for CO_2/SO_2, and 560 ± 140 for H_2O/HCl. Besides analytical uncertainties, the standard deviation on these ratios includes temporal fluctuations in the volcanic gas composition, as described thereafter. In Figs. 3c and 3d, the offset on the y-axis characterizes the respective air background amount of CO_2 (1.55×10^{20} molecules cm^{-2}) and H_2O (6.5×10^{21} molecules cm^{-2}) in the pit crater in the absence of any volcanic gas. The variable proportion (from 3% to 24%) of admixed volcanic gas implies significant temporal changes in the thickness of the measured volcanic layer. This is verified by computing the optical thickness of the purely atmospheric gas layer from the amount of N_2O in each spectrum: $L_a = (N_{N_2O}).T_a/(7.243 \times 10^{14}.P_a.[N_2O]_a)$, where $[N_2O]_a = 0.32$ ppmv and T_a and P_a are the ambient temperature and pressure. The average N_2O amount in all spectra, $(9.5 \pm 0.7) \times 10^{16}$ molecules cm^{-2}, constrains a mean atmospheric path length of 130 ± 10 m, somewhat lower than our measuring distance to the centre of the lake (140 ± 10 m), suggesting a mean thickness of order 10 m for the volcanic gas layer. However, the range in single air path values, from 100 to 160 m, demonstrates important fluctuations of the volcanic layer, in agreement with the pulsated degassing of the lava lake. The longest atmospheric paths, corresponding to low volcanic gas amounts, approach the slanting distance (170 m) between our measuring site and the southern wall of the pit behind the lava lake (Fig. 2); they thus indicate a thinned volcanic layer during transient episodes of reduced lake degassing. Instead, the shortest air paths correlate with both a higher gas temperature and a greater amount of total volcanic gas (a rough proxy for the gas flux), indicating a thicker volcanic layer and more intense lake degassing. On a few occasions, however, a thicker volcanic layer was an artefact due to backward turbulent transport of the volcanic gas cloud that, in addition to the targeted hot gases, was seen to cross the field of view of our spectrometer.

By subtracting the atmospheric background amounts discussed above, we thus obtain the air-corrected volcanic amounts of CO_2 and H_2O. For a finer air correction on much less abundant carbon monoxide, we combined the atmospheric path value derived from N_2O in each spectrum with Vanuatu's atmospheric CO content (0.07 ppmv) in October 2008. Fig. 4 depicts the time series of purely volcanic H_2O, CO_2, SO_2, HCl, HF and CO, as well as of the volcanic gas temperature and of the N_2O-based atmospheric path length. As expected, the temperature and the column amounts of volcanic gases display significant co-variations that are anti-correlated with changes in the atmospheric path length: the shorter the latter, the higher the former, and reciprocally.

3.2. Temporal variations in gas ratios

In contrast to gas column amounts, the volcanic gas ratios are insensitive to variable air dilution and thus track purely volcanic processes. Now, our data set reveals significant short-term fluctuations of the gas ratios (Figs. 5a–c) and hence of the bulk volcanic gas composition, which are well beyond the errors in our spectral retrievals. These variations reveal a highly dynamic degassing pattern of Benbow lava lake, as verified by the Morlet wavelet analysis of our data time series. Fig. 6 shows the wavelet periodograms for temperature and five selected gas ratios, while Fig. 7 depicts the

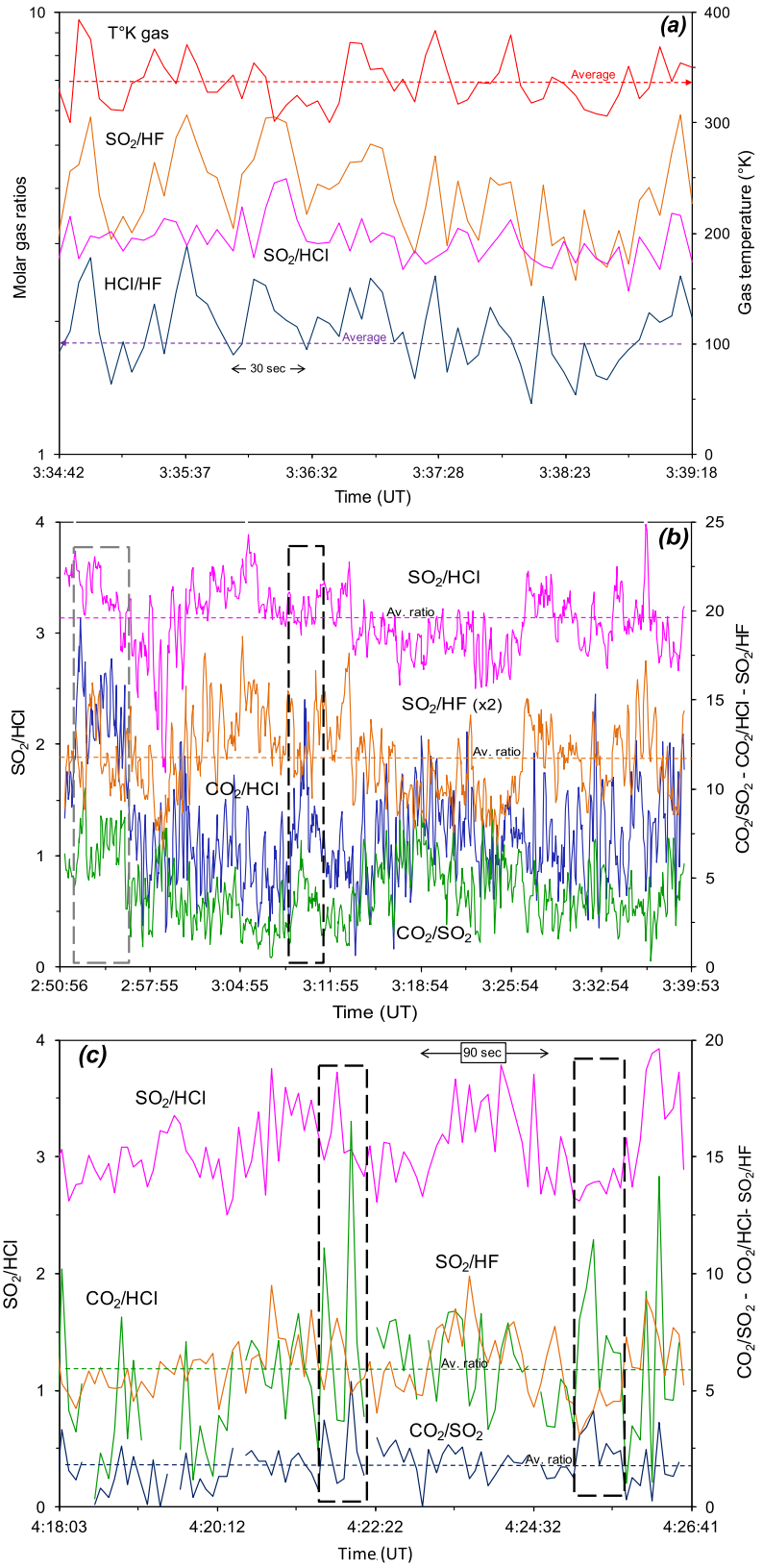

Fig. 5. Temporal variations of volcanic gas ratios during Benbow lava lake degassing: (a) SO_2/HF, HCl/HF, SO_2/HCl and gas temperature; SO_2/HCl, SO_2/HF, CO_2/HCl and CO_2/SO_2 ratios during (b) our first measuring sequence and during (c) an enlarged window of our second sequence. In Fig. 5a ratios are displayed on logarithmic scale to render HCl/HF oscillations more readable. In Fig. 5b data time series are fitted with a moving average of 15 s period (3 consecutive spectra). Framed time windows in Figs. 5b and 5c highlight the discrete CO_2 degassing events (high CO_2/HCl and CO_2/SO_2 at otherwise steady S/Cl/F ratios) corresponding to the bursting of meter-sized gas bubbles at the surface of the lava lake, which we attribute to the intermittent ascent and bursting of deeper-derived CO_2-rich large bubble or slugs in Benbow volcanic conduit (Section 4.2). See text for discussion.

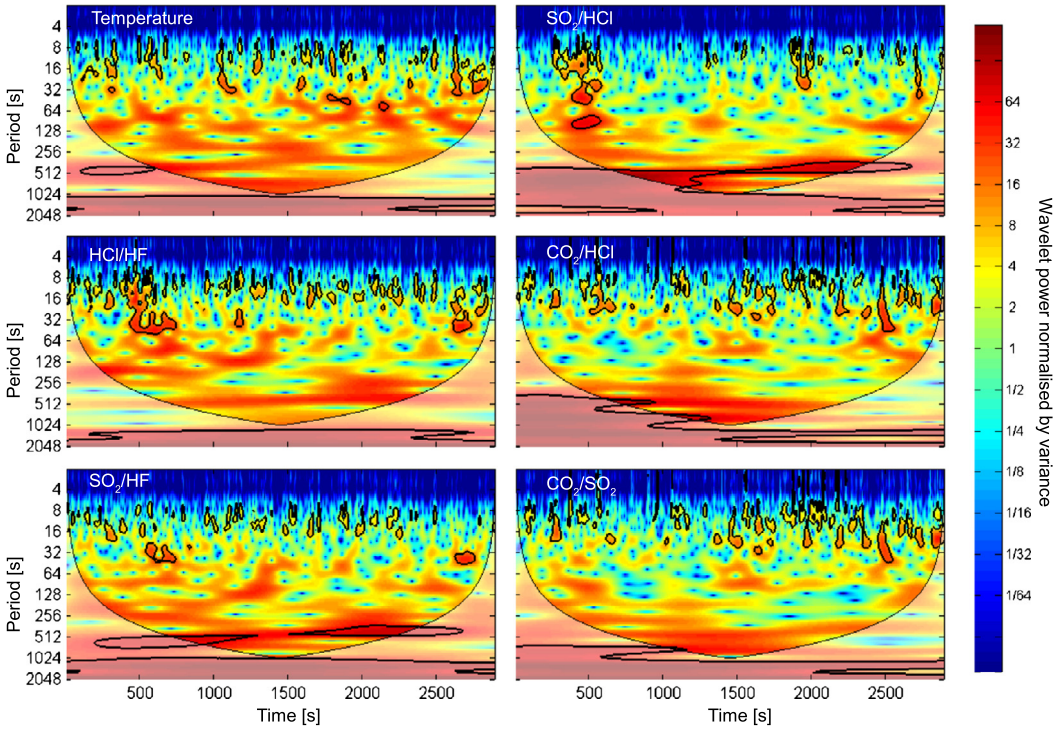

Fig. 6. Morlet wavelet periodograms of the volcanic gas temperature and five volcanic gas ratios (HCl/HF, SO_2/HF, SO_2/HCl, CO_2/HCl and CO_2/SO_2) over a 2885 s sampling time interval. Colour scale shows wavelet power normalised by variance. Black contours mark 95% confidence from the significance tests (Grinsted et al., 2004). Areas outside the cone of influence correspond to the edge effects from the wavelet (see section 2 for details). Two main degassing modulations appear: (i) recurrent short-period oscillations of T and most gas ratios in the band 8–32 s, sometimes extending up to 64 s, especially well defined for HCl/HF and SO_2/HF ratios; and (ii) a continuous long period modulation of all parameters at around 500-s (∼8 min), especially well defined by SO_2/HF and SO_2/HCl ratios. Results are discussed in section 4.2.

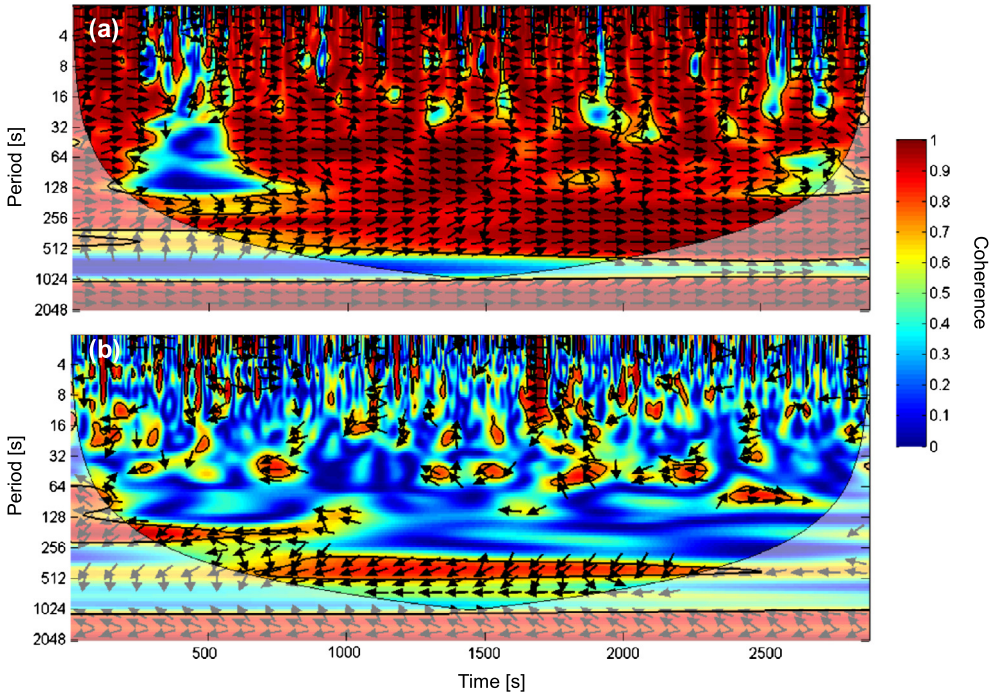

Fig. 7. Power spectra of wavelet coherence for two pairs of gas ratios: (a) SO_2/HF–HCl/HF and (b) CO_2/SO_2–HCl/HF. Colour scale defines the degree of coherence (1 for full correlation) and black lines delineate areas within 95% confidence level from Monte Carlo simulations. Arrows indicate the phase behaviour of the gas ratios: in phase (pointing right), out of phase (pointing left); first ratio leading (down), second ratio leading (up). A highly coherent behaviour is verified for SO_2/HF and HCl/HF at all times (except in the 250–750 s interval) and at all periods (though more pronounced in the bands 32–64 and 256–512 s). Instead, poor coherence exists between CO_2/SO_2 and HCl/HF, except at around 500 s periodicity and by intermittence in the band 8–64 s, and the two ratios are clearly shifted in phase owing to a prevalent distinct behaviour of CO_2/SO_2. See text for discussion.

wavelet coherence and phase relationship between (a) SO_2/HF and HCl/HF and (b) CO_2/SO_2 and HCl/HF. The following features arise from our results:

(i) Well defined short-period co-oscillations of the volcanic gas temperature and of most chemical ratios in the 8–32 s band, sometimes extended to about 64 s, that recur every ∼100 to 200 s (Fig. 6);
(ii) A continuous modulation of all parameters at around 500 s (∼8 min), especially well characterized by SO_2/HCl and SO_2/HF ratios (Fig. 6). Less well defined modulations also appear in the ∼100–250 s period band.
(iii) Close co-variations of both SO_2/HF and HCl/HF ratios with the volcanic gas temperature (Fig. 5a). Coherence tests (Fig. 7) verify a synchronous behaviour of these two gas ratios at all periods and at almost all times (except in the 250–750 s window). SO_2/HCl ratio broadly co-varies with SO_2/HF (Figs. 5b and 5c), especially at longer periodicity (Fig. 6), while displaying fewer apparent oscillations at short periods.
(iv) Both highly correlated and poorly correlated variations of CO_2/HCl and CO_2/SO_2 ratios with respect to both SO_2/HCl and SO_2/HF (Figs. 5b–c and 6). Coherence tests using HCl/HF as a reference do show a rare consistent behaviour of CO_2/SO_2 and HCl/HF ratios at short (8–64 s) and long (500 s) periods (Fig. 7), with a common phase shift (left-pointing arrows) prevalently due to CO_2/SO_2 (down-pointing arrows). In particular, our time series (Figs. 5b–c) reveal discrete spike increases of both CO_2/HCl and CO_2/SO_2 (by a factor 2 to 4) occurring at constant S/Cl/F ratios, which demonstrate intermittent episodes of selective CO_2 enrichment of the volcanic gas. Such events are outlined between 03:07:59 and 03:10:22 during our first measuring sequence (Fig. 5b) and between 04:21:51 and 04:22:20 during our second sequence (Fig. 5c). These CO_2 spikes, lasting from ∼1 to 2 min, were observed to coincide with the sequential bursting of very large (meter-sized) gas bubbles at the lake surface.

4. Discussion

4.1. Average composition of Benbow basaltic gas

From Fig. 3 and the air-corrected gas amounts in each spectrum we first derive the average molar composition of Benbow basaltic gas during our measurements. This composition (Table 1) is highly dominated by water vapour (96.1%), followed by CO_2 (2.2%), SO_2 (1.1%), HCl (0.35%), HF (0.19%) and CO (0.01%). Except for CO, reported here for the first time, we find that it is fairly comparable to the composition of cold Benbow plume emissions first analyzed with in situ methods in October 2007 (Allard et al., 2015). Despite completely different instrumental tools and data processing techniques, both data sets (Table 1) show closely similar H_2O content, SO_2/HCl (3.1 ± 0.4 versus 4.3 ± 1.7) and HCl/HF (1.9 ± 0.3 versus 2.3 ± 0.3) ratios, while possibly differing in a somewhat higher CO_2/SO_2 ratio in 2008 (2.0 ± 1.4) than 2007 (1.0 ± 0.2). This compositional resemblance for the same volcanic activity but at a one-year interval thus suggests quite steady magma degassing conditions. Long-term compositional gas stability at persistently active lava lakes, indicative of steady degassing processes, is a feature previously verified from repeated OP-FTIR measurements at Masaya (Burton et al., 2000), Nyiragongo (Sawyer et al., 2008a) and Erebus (Oppenheimer et al., 2009; Ilanko et al., 2015).

The CO/CO_2 ratio of Benbow volcanic gas, measured for the first time, averages 4.7×10^{-3} (Table 1). This ratio can be used to estimate the unknown redox conditions of Ambrym basaltic system if the gas equilibration temperature is determined.

Table 1
Molar composition of Ambrym's basaltic gas from Benbow lava lake in October 2008 and October 2007, compared with volcanic gases from other basaltic arc volcanoes and from lava lakes active in different geodynamic contexts.

Volcano	Measuring time	Geodynamic setting	Magma type	H_2O (mol %)	CO_2 (mol %)	SO_2 (mol %)	HCl (mol %)	HF (mol %)	CO (mol %)	H_2O/CO_2	CO_2/S	Cl/S	F/S	Method	Ref.
Benbow, Vanuatu	2008	Arc	basalt	96.2	2.2	1.1	0.35	0.19	0.003	44	2.0	0.32	0.17	FTIR	1
Ambrym[a], Vanuatu	2007	Arc	basalt	95.0	2.1	2.1	0.49	0.21	nd	45	1.0	0.23	0.10	in situ	2
Masaya, Nicaragua	1998–1999	Arc	basalt	94.2	3.3	1.4	0.86	0.19	bd	29	2.4	0.61	0.14	FTIR	3
Villarica, Chile	2009	Arc	bas. andesite	90.5	5.7	2.6	0.90	0.30	nd	16	2.2	0.35	0.12	FTIR	4
Villarica, Chile	2004	Arc	bas. andesite	95.0	2.0	2.1	0.63	0.23	nd	48	1.0	0.30	0.11	in situ	5
Miyakejima, Japan	2000?	Arc	basalt	94.9	2.0	2.7	0.24	nd	nd	47	0.7	0.09		in situ	6
Stromboli, Italy	2006	Arc	K-rich-basalt	82.9	13.6	1.7	1.7	bd	0.03	6.1	8.0	1.00		FTIR	7
Etna, Italy	2000	Cont. Margin	trachy basalt	92.0	7.3	1.0	0.10	0.07	0.004	12.6	7.3	0.10	0.07	FTIR	8
Erta Ale, Afar	1974	Rift	basalt	76.5	11.0	8.1	0.41	nd	0.54	7.0	1.4	0.05		in situ	9
Erta Ale, Afar	2005	Rift	basalt	93.6	3.7	2.5	0.19	0.04	0.06	26	1.5	0.08	0.02	FTIR	10
Kilauea, Hawaii	2004–05	Hot spot	basalt	81.8	6.4	10.7	1.1	0.45	0.05	13	0.6	0.10	0.04	FTIR	11
Kilauea, Hawaii	1940	Hot spot	basalt	59.9	32.2	7.8	0.05	nd	0.73	1.9	4.1	0.01		in situ	12
Erebus, Antarctica	2004	Cont. Rift	phonolite	57.9	36.4	1.4	0.69	1.27	2.3	1.6	26	0.49	0.91	FTIR	13
Nyiragongo, EAR	2005–2007	Cont. Rift	nephelinite	70.0	24.0	4.6	0.26	0.11	0.87	2.9	5.2	0.06	0.02	FTIR	14

Data sources: (1) This work; (2) Allard et al., 2015; (3) Burton et al., 2000; (4) Sawyer et al., 2011; (5) Shinohara and Witter, 2005; (6) Shinohara et al., 2003; (7) Burton et al., 2007a; (8) Allard et al., 2005; (9) Giggenbach and Le Guern, 1976; (10) Sawyer et al., 2008b; (11) Edmonds and Gerlach, 2007; (12) Gerlach and Graeber, 1985; (13) Oppenheimer and Kyle, 2008; (14) Sawyer et al., 2008a. EAR: East African Rift.
In situ = standard gas sampling/analysis methods. nd: not determined; bd: below detection.
[a] Mean composition of bulk Ambrym gas emissions from both Benbow and Marum craters in October 2007.

We assess this temperature from standard thermochemical data (Barin and Knacke, 1973) for the reaction: $3CO_2 + H_2S = 3CO + SO_2 + H_2O$, assuming ideal gas behaviour and combining the CO/CO_2 ratio and H_2O molar proportion (0.96) measured in 2008 with the SO_2/H_2S molar ratio of Benbow plume measured in 2007 with MultiGas sensors. The latter ranged between 10 (A. Aiuppa, pers. comm. 2007) and ≥100 (Allard et al., 2015). From these values we compute an apparent gas equilibrium temperature of between 1085 K and 1022 K at ambient pressure. This is much higher than the physical temperature of the volcanic gas (340 ± 20 K) derived from our FTIR spectra (section 3), demonstrating a relatively fast chemical quenching of the cooling magmatic gas phase after emission. From the equilibrium reaction $CO_2 = CO + 1/2O_2$ at 1022–1085 K and the CO/CO_2 ratio of Benbow gas, we then compute an oxygen fugacity of between −0.13 and +0.14 log-unit with respect to the NNO (nickel–nickel oxide) redox buffer. Therefore, we infer that the redox state of Ambrym basaltic system may be close to NNO, which is also typical for the parental basalt of Siwi–Yasur magmatic system in southern Vanuatu (Métrich et al., 2011) and, more broadly, for basaltic arc volcanism (e.g. Kelley and Cottrell, 2009).

4.2. Lava lake degassing pattern and mechanisms

Our OP-FTIR measurements performed at high temporal resolution and at short distance from Benbow lava lake provide unique insight into its degassing dynamics. The temporal variations in volcanic gas ratios reveal a highly dynamic degassing pattern (Figs. 5 and 6), involving both recurrent short-period (8–64 s) compositional oscillations, a longer-period (~8 min) continuous degassing modulation, and CO_2-rich discrete events coinciding with the bursting of large gas bubbles. Moreover, they reveal intervals of both coherence and incoherence between the gas ratios (Figs. 5 and 7), indicating the bearing of quite different physical processes at different times.

Because there is no permanent monitoring network on Ambrym, we cannot compare these high frequency geochemical variations with other (e.g. geophysical) parameters recorded synchronously. We therefore attempt to interpret them on basis of our field observations and melt inclusion data recently obtained for Ambrym arc basalt (Allard et al., 2015). The basalt was found to be moderately rich in volatiles (e.g. ~1.2 wt% H_2O and 0.1 wt% CO_2) and to prevalently degas in closed system upon ascent from a crustal reservoir emplaced at about 4 km beneath Benbow and Marum vents (Allard et al., 2015). Whereas CO_2 and sulphur start to exsolve at high pressures (~200 MPa and <150 MPa, respectively), H_2O, Cl and plausibly F (not analyzed) mainly exsolve at low to very low pressure during this process (Allard et al., 2015). These contrasted solubility behaviours in the melt are reflected in the P-related compositional evolution of the co-existing magmatic gas phase (Fig. 8), computed using VolatileCalc (Newman and Lowenstern, 2002) and the K_2O-normalized volatile content of the melt inclusions (see details in Fig. 8's caption). While a bulk magma degassing process well reproduces the average composition of Benbow volcanic gas, sharp variations of the total gas volume fraction, H_2O/CO_2 and S/Cl ratios result from the prominent degassing of H_2O and Cl at low pressures of between 25 and <10 MPa (Fig. 8). Below we use these observations to interpret the degassing pattern of Benbow lava lake.

We first notice that the recurrent (~100–200 s) short-period oscillations of Benbow gas temperature and composition (Fig. 6) match well the observed puffing activity of the lava lake. Their frequency, together with the relatively modest amplitude of variation of each parameter around its time-averaged value (Figs. 5a and 5c), point to a shallow degassing process sourced within the upper portion of the lava lake. We do interpret these recurrent short-term

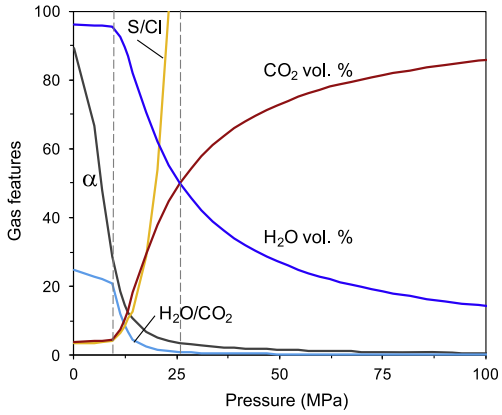

Fig. 8. Pressure-related compositional evolution of the magmatic gas phase during closed-system decompression of Ambrym arc basalt. The magmatic gas phase evolution was computed from the K_2O-normalised volatile content of olivine-hosted melt inclusions in Ambrym basalt (Allard et al., 2015), representative of the bulk basalt, and using VolatileCalc (Newman and Lowenstern, 2002) for the P-related degassing of H_2O and CO_2 at 1400 K from 220 MPa to the surface. K_2O varies from 1.85 wt% in the deepest, most primitive and volatile-richest inclusions (~1.2 wt% H_2O and 0.1 wt% CO_2) to 2.10–2.14 wt% in the matrix glass of Benbow erupted products, implying a slight magma differentiation upon ascent (Allard et al., 2015). Illustrated are evolutions of the total gas volume fraction (α), of the molar percentages of H_2O and CO_2 and of the molar S/Cl ratio in the magmatic gas phase. The cumulated exsolved amount of each volatile at every pressure step was computed by difference with respect to its initial dissolved content in the most primitive inclusions. A bulk magma degassing process well reproduces the average composition of Benbow volcanic gas. Note however the prominent degassing of both H_2O (H_2O/CO_2 increase) and Cl (sharp drop of S/Cl ratio) in the low-pressure range from 25 to <10 MPa, resulting in a marked increase of the total gas volume fraction and, hence, of the basalt vesicularity. See discussion in section 4.2.

variations as reflecting the periodic bursting of S-rich (high S/Cl and S/F ratios) and S-depleted (low S/Cl and S/F ratios) gas bubbles associated with the alternation, at the lake surface, of fresh lava blobs and partly degassed (S-depleted but still Cl–F-bearing), less hot lava. This interpretation is consistent with the modest amplitude of S/Cl fluctuations (from 2.5 to 4) around a mean value of 3.1 ± 0.4 (Fig. 3a), which imply a very shallow degassing process (Fig. 8). It also well accounts for the temporal changes in degassing intensity inferred from the anti-correlated variations in atmospheric path length and total volcanic gas amount (Fig. 4 and Section 3.1). In this framework, the ~100–200 s recurrence of the short-lived T-gas oscillations represents a time scale of convective resurfacing of the lava lake during our measurements.

Instead, the continuous modulation of almost all parameters with ~8 min period, especially well defined by SO_2/HCl and SO_2/HF ratios (Fig. 6), evidences a constant degassing periodicity of the volcanic system. Because it concerns all gas ratios this persistent dynamic signature likely typifies a somewhat deeper process involving both the lava lake and its feeder conduit. A plausible mechanism is the continuous influx of bubble-rich magma to the bottom of the lake, whose rate will determine the renewal time of the latter. The magma supply rate to Benbow crater was estimated to be as high as ~20 $m^3\,s^{-1}$ from the SO_2 flux emitted by this crater in October 2008 (see section 4.3) and from the magma sulphur content (Allard et al., 2015). If the degassing periodicity of ~8 min is taken to approximate the renewal time of the lava lake controlled by this supply rate, we infer a lake volume of ~10^4 m^3, about twice that of Erebus lava lake (Oppenheimer et al., 2009).

Finally, we invoke a deeper, conduit source for the discrete CO_2 degassing events characterized by sharp spike increases of CO_2/HCl and CO_2/SO_2 at constant S/Cl/F ratios (Figs. 5b and 5c). The chemical amplitude of these intermittent events, their duration (~1–2 min) and their coincidence with the bursting of series of meter-sized bubbles at the lake surface strongly suggest the separate ascent, in Benbow conduit, of large gas bubbles or slugs

preferentially enriched in early exsolved CO_2 (Fig. 8). This means that, despite prevalent closed-system degassing of the basalt upon ascent, bubble accumulation and modest coalescence would also occur at some depth in the feeding system. A quantitative estimate is however impossible at present owing to the natural lack of CO_2-bearing melt inclusions trapped at less than ~75 MPa (Allard et al., 2015).

The diameter of Benbow conduit can tentatively be estimated from the magma supply rate of ~20 $m^3 s^{-1}$ mentioned above. Extensive convection in Benbow feeding system, with downward recycling of the denser degassed magma, is required to accommodate for such a rate, little of which exits as lava clots and ash (Allard et al., 2015). Magma convection is also supported by the textural features of Benbow eruptive products (Polacci et al., 2012). Here we focus on the uppermost conduit, assumed to be vertical and cylindrical for the sake of simplicity. As shown by Beckett et al. (2014), the net volumetric flux (Q) of magma upraising in a vertical conduit with bi-directional exchange flow does not depends on the flow regime and can be approximated by the following relationship:

$$Q = 0.059\beta^{-0.74}\left(\frac{g\Delta\rho R^4}{2\mu_b}\right)$$

where β is the viscosity ratio between the degassed and the volatile-rich buoyant magma components, $\Delta\rho$ is their difference in density, μ_b is the dynamic viscosity of the buoyant component, g is gravitational acceleration and R is the effective conduit radius. We use the rhyolite-MELTS + H_2O–CO_2 software (version 1.2.x; Ghiorso and Gualda, 2015) to compute magma densities and viscosities at a temperature of 1400 K which, under NNO redox conditions (such as inferred in section 4.1), well accounts for the melt composition, the low crystal content (<5 to 10%) and the mineral chemistry of Benbow products (Allard et al., 2015; N. Métrich, unpub. data, 2012; Picard et al., 1995). As shown in Fig. 8, during its closed-system ascent Ambrym basalt will reach 50% vesicularity – a threshold for permeability-controlled gas percolation and hence open degassing (Burton et al., 2007b) – while decompressing to less than 10 MPa. Under these conditions the buoyant magma has a density of ~1500 kg m^{-3} and an effective viscosity of 595.5 Pa s if one assumes spherical-shaped bubbles and a low capillary number (Pal, 2002). Once degassed at or near the surface of the lake, the magma becomes much denser (2700 kg m^{-3}) and more viscous (1445 Pa s) and, therefore, should rapidly sink down the lake and the feeder conduit. From these numbers and the above equation we compute a diameter of 6 ± 1 m for Benbow upper conduit, taking account of propagating uncertainties on the different parameters. Before entering the lava lake, the buoyant basalt would flow at 1.4 m s^{-1} across the inner half section of the conduit, which is a favourable condition to maintain bubble–melt coupling up to very shallow depth.

Finally, we emphasize that the degassing pattern of a vigorously active basaltic lake on Ambrym markedly differs from that recorded during quieter lava lake activity at either Erebus or Kilauea, the only two volcanoes where detailed OP-FTIR investigations have been achieved until now. At Erebus, passive degassing with relatively constant composition was found to prevail between the explosive bursting of deeper-derived large gas bubbles or slugs happening every ~10 mn (Oppenheimer et al., 2009; Ilanka et al., 2015), while at Kilauea ~30 mn long cycles of low passive degassing and lava lake upheaval, controlled by shallow bubble accumulation (gas pistoning), were observed to alternate with intervals of spattering and increased H_2O–SO_2-rich gas release after a sudden drop in lake level (Patrick et al., 2016). With an estimated volume of 10^4 m^3, an upper (surface) diameter of ~ 25 m and a lower (conduit) diameter of ~6 m, Benbow lava lake (as an inverted truncated cone) would have had a modest height of ~12 m in October 2008. Such small dimensions, coupled with the high basalt supply rate of ~20 $m^3 s^{-1}$, well explain its vigorous degassing and rapid renewal rate. Instead, the much quieter degassing patterns of lava lakes at Kilauea and Erebus is fully consistent with their longer renewal rate (about 4 days and 4 h, respectively; Patrick et al., 2016; Oppenheimer et al., 2009), due to a lower magma supply rate but also a much larger size for Kilauea basaltic lake (2.5×10^6 m^3 and 100 m deep in 2010; Carbone et al., 2013) and a much higher viscosity in case of Erebus phonolite lake (Oppenheimer et al., 2009).

4.3. Ambrym volcanic gas composition and emission rates compared with other lava lakes worldwide

Ambrym basaltic gas from Benbow lava lake in October 2008 is compared in Table 1 with magmatic gases from other active lava lakes measured with OP-FTIR spectroscopy and/or classical (in situ) methods. Ambrym basaltic gas is markedly richer in water and halogens than hot spot or rift basaltic gases from Kilauea and Erta'Ale lava lakes, respectively, whilst being poorer in CO_2 than magmatic gases from Nyiragongo and Erebus alkaline lakes. These features are coherent with differences in magma compositions and geodynamic contexts. Ambrym volcanic gas more closely resembles arc volcanic gases from Masaya (Burton et al., 2000) and Villarrica (Sawyer et al., 2011) lava lakes (Table 1) and typically plots within the compositional field for arc volcanism for both major components and trace halogen species (Allard et al., 2015).

Airborne DOAS measurements on 8 October 2008 revealed a total SO_2 plume flux of $\sim 100 \pm 30$ kg s^{-1} from the volcano, 75% of which arose from Benbow and 25% from Marum craters (Allard et al., 2015). Combining the specific SO_2 flux from Benbow (~75 kg s^{-1}, or 6500 Mg d^{-1}) with the average gas composition measured with OP-FTIR spectroscopy (Table 1), we compute the simultaneous emission of 1.6×10^5 Mg d^{-1} of H_2O, 9×10^3 Mg d^{-1} of CO_2, 1.2×10^3 Mg d^{-1} of HCl, 350 Mg d^{-1} of HF and 8 Mg d^{-1} of CO (with overall ±30% uncertainty; Table 2). Such gas emission rates are far larger than those from most other lava lakes. For instance, Benbow fluxes of H_2O, HCl and HF exceed by factors as high as 190–670, 50–460 and 17–1000 the ranges in corresponding fluxes from Erebus, Kilauea and Erta'Ale lava lakes (Table 2). In terms of H_2O, CO_2 and SO_2 fluxes, whose sum approximates the total gas flux, Benbow crater (and Ambrym as a whole) is of comparable strength as Nyiragongo (Sawyer et al., 2008a), despite widely differing magma compositions. The CO_2 discharge of ~10 Gg per day from Benbow in October 2008 actually ranks amongst the highest known emissions of igneous carbon from persistently degassing volcanoes (Burton et al., 2013). As a matter of fact, our study provides further evidence that Ambrym volcano ranks among the top-three persistent emitters of magma-derived volatiles at a global scale, together with Nyiragongo and Etna (Table 2). In addition to their impact on local ecosystems (Bani et al., 2009; Allibone et al., 2012), volcanic gas emissions from Ambrym may thus have a considerable atmospheric impact at regional scale in the southwest Pacific (Lefèvre et al., in press).

5. Conclusions

We performed the first OP-FTIR measurements of gas emissions from Benbow crater on Ambrym volcano, in Vanuatu. Ambrym is one of the rare basaltic arc volcanoes displaying persistent lava lake activity, but has long remained undocumented for its degassing compared to other, more accessible lava lakes worldwide. We measured gas absorption spectra at short range (~140 m) using the vigorously active Benbow lava lake itself as a radiation source. Analysis of these spectra allowed retrieval of volcanic H_2O,

Table 2
Gas emission rates from Benbow crater in 2008 and Ambrym in 2007, compared to gas emissions rates from other active lava lakes worldwide.

Volcano	Measuring time	H_2O ($Mg\,d^{-1}$)	CO_2 ($Mg\,d^{-1}$)	SO_2 ($Mg\,d^{-1}$)	HCl ($Mg\,d^{-1}$)	HF ($Mg\,d^{-1}$)	CO ($Mg\,d^{-1}$)	Total gas ($Mg\,d^{-1}$)	Ref.
Benbow, Vanuatu	2008	1.6×10^5	9×10^3	6500	1200	350	8.0	2.1×10^5	1
Ambrym, Vanuatu	2007	1.1×10^5	1.4×10^4	7800	1100	240	nd	1.3×10^5	2
Masaya, Nicaragua	1998–1999	3.5×10^4	2900	1800	640	78	nd	4.0×10^4	3
Villarrica, Chile	2009	3100	480	315	60	11	nd	4.0×10^3	4
Erta 'Ale, Afar	2005	630	60	60	2.6	0.4	0.7	7.5×10^2	5
Kilauea, Hawaii	2009	240	80	900	23	10	nd	1.3×10^3	6
Erebus, Antarctica	2004	860	1330	75	21	21	54	2.4×10^3	7
Nyiragongo, EAR	2005	1.5×10^5	1.2×10^4	3300	105	26	285	2.7×10^5	8

Data sources: (1) This work; (2) Allard et al., 2015, bulk Ambrym emissions; (3) Burton et al., 2000; (4) Sawyer et al., 2011; (5) Sawyer et al., 2008b; (6) Edmonds et al., 2013; (7) Oppenheimer and Kyle, 2008; (8) Sawyer et al., 2008a.

CO_2, SO_2, HCl, HF and CO path amounts at high temporal resolution (5 s period). Our gas composition data were combined with simultaneously measured SO_2 fluxes to quantify fluxes for each measured magmatic gas species from Ambrym.

We outline the following main observations:

(i) Lava lake degassing at Ambrym clearly differs in its water-halogen-rich average composition from basaltic or alkaline volcanic gases from long-lived lava lakes on rifting plate boundaries (Erta'Ale, Nyiragongo, Erebus) or hot spots (Kilauea). It more closely resembles volcanic gases from other basaltic arc volcanoes, in agreement with Ambrym' subduction zone setting.

(ii) Temporal variations of Benbow volcanic gas composition during our measuring interval reveal a highly dynamic degassing pattern of the lava lake. Short-period oscillations of most ratios, recurring every ~100–200 s, match the observed pulsated degassing (puffing) of the lake. These oscillations, especially clear and coherent for SO_2/HF, HCl/HF and SO_2/HCl ratios and correlated with temperature variations, indicate an inside-lake shallow degassing process marked by the periodic bursting of S-rich (high S/Cl ratio) and S-depleted (low S/Cl) gas bubbles associated with the alternation of fresh lava and degassed lava at the lake surface. A longer-period (~8 min) persistent modulation of the gas ratios, particularly well characterized for SO_2/HF and SO_2/HCl, probably tracks the influx of bubble-rich magma at the bottom of the lake and thus the rate of convective renewal of this latter. Occasional sharp increases of CO_2/HCl and CO_2/SO_2 at constant S/Cl/F ratios, lasting 1–2 min, evidence discrete degassing events during which carbon dioxide was selectively enriched in the emitted gas. These events, coinciding with the bursting of meter-sized bubbles at the lake surface, are attributed to the separate ascent of deeper derived (CO_2-rich) large gas bubbles or slugs in Benbow feeder conduit, the diameter of which is estimated as 6 ± 1 m.

(iii) The highly dynamic degassing pattern of Benbow basaltic lake markedly differs from that of quieter lava lakes at either Kilauea or Erebus. In first order, this can be related to a smaller size and much faster renewal rate of Benbow lava lake, due to a very high basalt supply rate, compared to Kilauea basaltic lake, and to a much lower magma viscosity when compared to the phonolite lake of comparable size occurring at Erebus.

(iv) Gas emission rates from Benbow crater in October 2008 include 160 $Gg\,d^{-1}$ of H_2O, ~10 $Gg\,d^{-1}$ of CO_2 and ~8 $Gd\,d^{-1}$ of total acid gases (SO_2, HCl and HF). Such emission rates are far larger than those from other lava lakes currently active worldwide, with the exception of Nyiragongo lava lake on the East African rift. We further verify that Ambrym volcano actually ranks amongst the three most powerful persistent emitters of volcanic gases at global scale and, hence, may have a considerable environmental impact in the southwest Pacific region.

Our study of lava lake degassing on Ambrym arc volcano further illustrates the great potential of OP-FTIR spectroscopy to investigate magma degassing processes at high temporal resolution. It reveals an unprecedented dynamism in gas emissions from a basaltic lake, reflecting the superimposed processes of coupled and decoupled ascent of magma and gas which feed this remarkable volcanic system. Such new insights into shallow magma dynamics at a highly active basaltic volcano provide a valuable basis for quantitative interpretation and modelling of gas composition variations and magma dynamics at other lava lakes and open-vents basaltic volcanoes.

Acknowledgements

Our study was supported by the French National Research Agency, through 2007–2010 contracts "VOLGASPEC" (06-CATT-012-01) and "Arc Vanuatu" (06-CATT-012-002), and benefited from funding from the European Research Council (FP/2007-2013/ERC Grant Agreement No. 279802). We acknowledge B. Pelletier (IRD, Noumea), E. Garaebiti (GEOHAZARD, Vanuatu), guides and porters from Ambrym's Lalinda village for local assistance, and G. Tamburello (Palermo University, Italy) for its help in Morlet wavelet analysis. Thorough reviews by K. Iacovino, M. Patrick and two anonymous referees, as well as careful editing by T. Mather, greatly improved our manuscript.

References

Allard, P., Burton, M., Murè, F., 2005. Spectroscopic evidence for a lava fountain driven by previously accumulated magmatic gas. Nature 43 (7024), 407–410.

Allard, P., Aiuppa, A., Bani, P., Métrich, N., Bertagnini, A., Gauthier, P-J., Shinohara, H., Sawyer, G., Parello, F., Bagnato, E., Pelletier, B., Garaebiti, E., 2015. Prodigious emission rates and magma degassing budget of major, trace and radioactive volatile species from Ambrym basaltic volcano, Vanuatu island Arc. J. Volcanol. Geotherm. Res. http://dx.doi.org/10.1016/j.jvolgeores.2015.08.022. Special issue on Vanuatu Volcanoes.

Allibone, R., Cronin, S.J., Charley, D.T., Neall, V.E., Stewart, R.B., Oppenheimer, C., 2012. Dental fluorosis linked to degassing of Ambrym volcano, Vanuatu: a novel exposure pathway. Environ. Geochem. Health 34 (2), 155–170. http://dx.doi.org/10.1007/s10653-010-9338-2.

Bani, P., Oppenheimer, C., Tsanev, V.I., Carn, S.A., Cronin, S.J., Crimp, R., Charley, D., Lardy, M., Roberts, T.R., 2009. Surge in sulphur and halogen degassing from Ambrym volcano, Vanuatu. Bull. Volcanol. 71 (10), 1159–1168. http://dx.doi.org/10.1007/s00445-009-0293-7.

Bani, P., Oppenheimer, C., Allard, P., Shinohara, H., Lardy, M., Garaebiti, E., 2012. First estimate of volcanic SO_2 budget for Vanuatu island arc. J. Volcanol. Geotherm. Res. 211–212, 36–46. http://dx.doi.org/10.1016/j.jvolgeores.2011.10.005.

Barin, I., Knacke, O., 1973. Thermochemical Properties of Inorganic Substances. Springer-Verlag, Berlin. 921 pp.

Beckett, F.M., Burton, M., Mader, H.M., Phillips, J.C., Polacci, M., Rust, A.C., Witham, F., 2014. Conduit convection driving persistent degassing at basaltic volcanoes. J. Volcanol. Geotherm. Res. 283, 19–35. http://dx.doi.org/10.1016/j.jvolgeores.2014.06.006.

Bouche, E., Vergniolle, S., Staudacher, T., Nercessian, A., Delmont, J.-C., Frogneux, M., Cartault, F., Le Pichon, A., 2010. The role of large bubbles detected from acoustic measurements on the dynamics of Erta 'Ale lava lake (Ethiopia). Earth Planet. Sci. Lett. 295, 37–48.

Burton, M., Oppenheimer, C., Horrocks, L.A., Francis, P.W., 2000. Field measurement of CO_2 and H_2O emissions from Masaya Volcano, Nicaragua, by Fourier transform spectrometry. Geology 28, 915–918.

Burton, M., Allard, P., Murè, F., La Spina, A., 2007a. Magmatic gas composition reveals the source depth of slug-driven Strombolian explosive activity. Science 317 (5835), 227–230. http://dx.doi.org/10.1126/science.114190.

Burton, M.R., Mader, H.M., Polacci, M., 2007b. The role of gas percolation in quiescent degassing of persistently active basaltic volcanoes. Earth Planet. Sci. Lett. 264 (1–2), 46–60. http://dx.doi.org/10.1016/j.epsl.2007.08.028.

Burton, M., Sawyer, G.M., Granieri, D., 2013. Deep carbon emissions from volcanoes. Rev. Mineral. Geochem. 75, 323–354.

Carbone, D., Poland, M.P., Patrick, M.R., Orr, T.R., 2013. Continuous gravity measurements reveal a low-density lava lake at Kilauea Volcano, Hawaii. Earth Planet. Sci. Lett. 376, 178–185.

Commonwealth Scientific and Industrial Research Organisation (CSIRO) Australia, October 2008. http://www.csiro.au/greenhouse-gases/, ftp://gaspublic:gaspublic@ftp.dar.csiro.au/data/gaslab/.

Edmonds, M., Gerlach, T.M., 2007. Vapor segregation and loss in basaltic melts. Geology 35 (8), 751–754.

Edmonds, M., Sides, I.R., Swanson, D.A., Werner, C., Martin, R.S., Mather, T.A., Herd, R.A., Jobes, R.L., Mead, M.I., Sawyer, G., Roberts, T.J., Sutton, A.J., Elias, T., 2013. Magma storage, transport and degassing during the 2008–10 summit eruption at Kilauea volcano, Hawaii. Geochim. Cosmochim. Acta 123, 284–301. http://dx.doi.org/10.1016/j.gca.2013.05.038.

Edwards, D.J., Dudhia, A., 1996. Reference forward model: high level algorithms definition. ESA document PO-MA-OXF-GS-0004.

Gerlach, T.M., Graeber, E.J., 1985. Volatile budget of Kilauea volcano. Nature 313, 273–277.

Ghiorso, M.S., Gualda, G.A.R., 2015. An H_2O–CO_2 mixed fluid saturation model compatible with rhyolite-MELTS. Contrib. Mineral. Petrol. 169, 53. http://dx.doi.org/10.1007/s00410-015-1141-8.

Giggenbach, W.F., Le Guern, F., 1976. The chemistry of magmatic gases from Erta 'Ale, Ethiopia. Geochim. Cosmochim. Acta 40, 25–30.

Grinsted, A., Moore, J.C., Jevrejeva, S., 2004. Application of the cross wavelet transform and wavelet coherence to geophysical time series. Nonlinear Process. Geophys. 11, 561–566. http://dx.doi.org/10.5194/npg-11-561-2004.

Harris, A.J.L., Flynn, L.P., Rothery, D.A., Oppenheimer, C., Sherman, S.B., 1999. Mass flux measurements at active lava lakes: implications for magma recycling. J. Geophys. Res. 104, 7117–7136.

Ilanko, T., Oppenheimer, C., Burgisser, A., Kyle, P., 2015. Cyclic degassing of Erebus volcano, Antarctica. Bull. Volcanol. 77, 56–71. http://dx.doi.org/10.1007/s00445-015-0941-z.

Kazahaya, K., Shinohara, H., Saito, G., 1994. Excessive degassing of Izu-Oshima volcano: magma convection in a conduit. Bull. Volcanol. 56, 207–216.

Kelley, K.A., Cottrell, E., 2009. Water and the oxidation state of subduction zone magmas. Science 925 (5940), 605–607. http://dx.doi.org/10.1126/science.1174156.

La Spina, A., Burton, M., Allard, P., Alparone, S., Murè, F., 2015. Open-path FTIR spectroscopy of magma degassing processes during eight lava fountains on Mount Etna. Earth Planet. Sci. Lett. 413, 123–134. http://dx.doi.org/10.1016/j.epsl.2014.12.038.

Lefèvre, J., Menkes, C., Bani, P., Marchesiello, P., Curci, G., Grell, G.A., Frouin, R., in press. Distribution of sulfur aerosol precursors in the SPCZ released by continuous volcanic degassing at Ambrym, Vanuatu. J. Volcanol. Geotherm. Res. http://dx.doi.org/10.1016/j.jvolgeores.2015.07.018.

Le Guern, F., Carbonnelle, J., Tazieff, H., 1979. Erta 'Ale lava lake: heat and gas transfer to the atmosphere. J. Volcanol. Geotherm. Res. 6, 27–48.

MacCall, G.J.H., Le Maitre, R.W., Madoff, A., Robinson, G.P., Stephenson, P.J., 1970. The geology and geophysics of the Ambrym caldera, New Hebrides. Bull. Volcanol. 34, 681–696.

Métrich, N., Allard, P., Aiuppa, A., Bani, P., Bertagnini, A., Belhadj, O., Di Muro, A., Garaebiti, E., Massare, D., Parello, F., Shinohara, H., 2011. Magma and volatile supply to post-collapse volcanism and block resurgence in Siwi caldera (Tanna island, Vanuatu arc). J. Petrol. 52, 1077–1105. http://dx.doi.org/10.1093/petrology/egr019.

Moussallam, Y., Oppenheimer, C., Scaillet, B., Buisman, I., Kimball, C., Dunbar, N., Burgisser, A., Schipper, C.I., Andújar, J., Kyle, P., 2015. Megacrystals track magma convection between reservoir and surface. Earth Planet. Sci. Lett. 413, 1–12. http://dx.doi.org/10.1016/j.epsl.2014.12.022.

Newman, S., Lowenstern, J.B., 2002. VolatileCalc: a silicate melt–H_2O–CO_2 solution model written in Visual Basic for excel. Comput. Geosci. 28, 597–604.

Oppenheimer, C., McGonigle, A.J.S., Allard, P., Wooster, M.J., Tsanev, V., 2004. Sulfur, heat, and magma budget of Erta 'Ale lava lake, Ethiopia. Geology 32 (6), 509–512.

Oppenheimer, C., Kyle, P.R., 2008. Probing the magma plumbing of Erebus volcano, Antarctica, by open-path FTIR spectroscopy of gas emissions. J. Volcanol. Geotherm. Res. 177 (3), 743–754. http://dx.doi.org/10.1016/j.jvolgeores.2007.08.022.

Oppenheimer, C., Lomakina, A.S., Kyle, P.R., Kingsbury, N.G., Boichu, M., 2009. Pulsatory magma supply to a phonolite lava lake. Earth Planet. Sci. Lett. 284, 392–398. http://dx.doi.org/10.1016/j.epsl.2009.04.043.

Pal, R., 2002. Rheological behaviour of bubble-bearing magmas. Earth Planet. Sci. Lett. 207, 165–179.

Patrick, M.R., Orr, T., Sutton, A.J., Lev, E., Thelen, W., Fee, D., 2016. Shallow driven fluctuations in lava lake outgassing (gas pistoning), Kilauea volcano. Earth Planet. Sci. Lett. 433, 326–338. http://dx.doi.org/10.1016/j.epsl.2015.10.052.

Picard, C., Monzier, M., Eissen, J.-P., Robin, C., 1995. Concomitant evolution of tectonic environment and magma geochemistry, Ambrym volcano (Vanuatu, New Hebrides arc). In: Smellie, J.L. (Ed.), Volcanism Associated with Extension at Consuming Plate Margin. Geol. Soc. America, Special Pub., pp. 135–154.

Polacci, M., Baker, D.R., La Rue, A., Mancini, L., Allard, P., 2012. Degassing behaviour of vesiculated basaltic magmas: an example from Ambrym volcano, Vanuatu Arc. J. Volcanol. Geotherm. Res. 233–234, 55–64. http://dx.doi.org/10.1016/j.jvolgeores.2012.04.019.

Rodgers, C.D., 1976. Retrieval of atmospheric temperature and composition from remote measurements of thermal radiation. Rev. Geophys. 14 (4), 609–624.

Rothman, L.S., et al., 2005. The HITRAN 2004 molecular spectroscopic database. J. Quant. Spectrosc. Radiat. Transf. 96 (2), 139–204.

Sawyer, G.M., Carn, S.A., Tsanev, V., Oppenheimer, C., Burton, M., 2008a. Investigation into magma degassing at Nyiragongo volcano, Democratic Republic of the Congo. Geochem. Geophys. Geosyst. 9 (2), Q02017. http://dx.doi.org/10.1029/2007GC001829.

Sawyer, G.M., Oppenheimer, C., Tsanev, V.I., Yirgu, G., 2008b. Magmatic degassing at Erta'Ale volcano, Ethiopia. J. Volcanol. Geotherm. Res. 187, 837–846. http://dx.doi.org/10.1016/j.jvolgeores.2008.09.017.

Sawyer, G.M., Salerno, G., Le Blond, J.S., Martin, R.S., Spampinato, L., Roberts, T.J., Mather, T.A., Witt, M.L.I., Tsanev, V.I., Oppenheimer, C., 2011. Gas and aerosol emissions from Villarrica volcano, Chile. J. Volcanol. Geotherm. Res. 203, 62–75. http://dx.doi.org/10.1016/j.jvolgeores.2011.04.003.

Shinohara, H., Witter, J.B., 2005. Volcanic gases emitted during mild Strombolian activity of Villarrica volcano, Chile. Geophys. Res. Lett. 32, L20308. http://dx.doi.org/10.1029/2005GL024131.

Shinohara, H., Fukui, K., Kazahaya, K., Saito, G., 2003. Degassing process of Miyakejima volcano: implications of gas emission rate and melt inclusion data. In: De Vivo, B., Bodnar, B. (Eds.), Melt Inclusions in Volcanic Systems. In: Dev. Volcanol. Ser., vol. 5. Elsevier, New York, pp. 147–161.

Stevenson, D.S., Blake, S., 1998. Modelling the dynamics and thermodynamics of volcanic degassing. Bull. Volcanol. 60, 307–317.

Tamburello, G., Aiuppa, A., Mcgonigle, A.J.S., Allard, P., Cannata, A., Kantzas, E.P., 2013. Periodic volcanic degassing behavior: Mount Etna example. Geophys. Res. Lett. 40, 4818–4822. http://dx.doi.org/10.1002/grl.50924.

Tazieff, H., 1994. Permanent lava lakes: observed facts and induced mechanisms. J. Volcanol. Geotherm. Res. 63, 3–11. http://dx.doi.org/10.1016/0377-0273(94)90015-9.

Torrence, C., Compo, G.P., 1998. A practical guide to wavelet analysis. Bull. Am. Meteorol. Soc. 79, 61–78. http://dx.doi.org/10.1175/1520-0477(1998)079%3C0061:APGTWA%3E2.0.CO;2.

Witham, F., Llewellin, E.W., 2006. Stability of lava lakes. J. Volcanol. Geotherm. Res. 158, 321–332. http://dx.doi.org/10.1016/j.jvolgeores.2006.07.004.